Inductive effects on energy–harvesting piezoelectric flag

Y. Xia[a], S. Michelin[a], O. Doaré[b]

a. *LadHyX–Département de Mécanique, École Polytechnique, Route de Saclay, 91128 Palaiseau, France*

b. *ENSTA, Paristech, Unité de Mécanique (UME), Chemin de la Hunière, 91761 Palaiseau, France*

Résumé :

L'interaction d'un drapeau flexible avec un écoulement donne lieu à une instabilité fluide–structure classique qui conduit à une vibration auto-entretenue, dont l'énergie mécanique peut être convertie en énergie électrique par le biais de matériaux piézoélectriques qui couvrent le drapeau et se déforment avec celui-ci. On étudie la possibilité de récupérer cette énergie, et en particulier l'effet d'un circuit inductif sur le processus de récupération. Une déstabilisation du système est observée par l'ajout d'une inductance. En régime non-linéaire, l'efficacité de récupération augmente significativement lors de l'accrochage entre les fréquences de battement du drapeau et du circuit électrique.

Abstract:

Interaction between a flexible flag and a flow leads to a canonical fluid–structure instability which produces self-sustained vibrations, from which mechanical energy could be converted to electrical energy through piezoelectric materials covering the flag and thus being deformed by its motion. We study the possibility of harvesting this energy, especially the effect of an inductive circuit on the energy harvesting process. A destabilization of the coupled system is observed after adding an inductance. In the nonlinear case, the harvesting efficiency increases significantly at lock–in between the frequencies of the fluttering flag and the electrical circuit.

Mots clefs : **piezo–electricity ; energy harvesting ; lock–in**

1 Introduction

The limited availability of exploitable fossil energy resources urges increasing effort to be invested on the development of renewable energy. The omnipresence and low environmental impact make geophysical flows (e.g. tidal currents, winds, etc.) a promising energy source. Classical phenomena in fluid–solid interaction, such as vortex-induced vibrations and flag flutter, are interesting candidates of flow energy harvesting mechanisms as these interactions may result in self–sustained vibrations of the solid in an uniform flow, thus permanent energy transfer between the fluid flow and the solid.

Piezoelectric materials are known for their capability of generating electrical charge when being deformed. The periodic deformation of the flag therefore leads to a periodic charge transfer between the electrodes of piezoelectric patches positioned on the flag's surface. The feasibility and performance of harvesting the electrical charge by a resistive circuit was recently studied[3, 7], and it was shown that both the stability of the system and the fluttering dynamics are influenced by electrical coupling.

Based on these works, we are interested in a slightly more complicated electric coupling : a resistive–inductive (RL) output circuit. Adding inductive elements to a purely passive circuit allows the latter to have its own dynamical properties, in particular a natural frequency, and therefore the possibility of resonance with the flapping flag. Both linear stability and nonlinear dynamics of the coupled fluid–solid–electric system are studied. In this article, some results are presented in attempt to attract readers' attention to several significant influences brought to the coupled system by adding an inductance to the output circuit.

2 Modeling of the coupled system

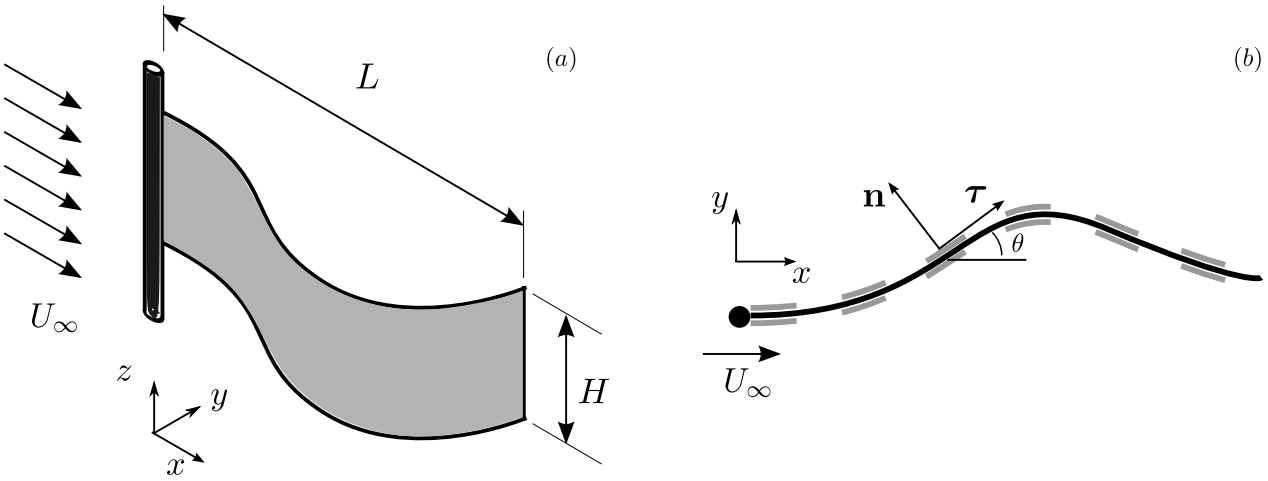

FIGURE 1 – (a)Flapping piezoelectric flag in a uniform axial flow and (b) its 2 dimensional view. Piezoelectric patches are represented by gray strips in (a) and segments in (b)

The coupled fluid–structure system considered here is a cantilevered flag placed in an axial flow, which is illustrated in figure 1. Assuming the flag is inextensible with 2–dimensional movement in the (x, y) plane, its dynamics can be described using an Euler–Bernoulli beam model. Lighthill's *Large Amplitude Elongated Body Theory* (LAEBT)[6] is used to calculate the force resulting from the fluid added mass[4][7]. The effect of crossflow separation is modeled by taking into account a drag in the fluid forcing expression, as proposed in [4].

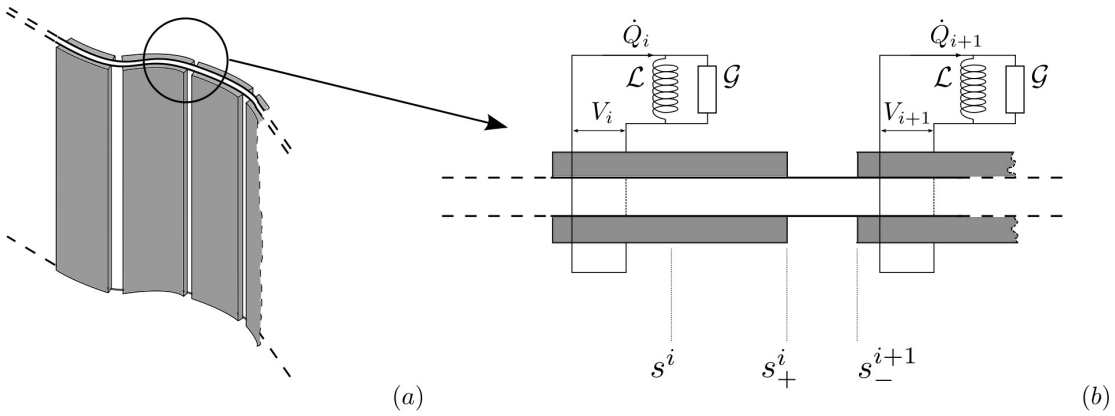

FIGURE 2 – (a) Flag shunted with piezoelectric pairs. The junction between two adjacent pairs are detailed in (b)

As shown in figure 2, the surface of the flag is entirely covered by pairs of piezoelectric patches of length d in the flow direction. The resulting three–layer sandwich plate is of lineic mass μ and bending rigidity B. Each pair is shunted with a conductance $\mathcal{G}$ and an inductance $\mathcal{L}$, which are connected in parallel. Q and V are respectively electrical charge and voltage resulting from the piezoelectric effects.

Following[3][7], we assume that piezoelectric pairs are continuously distributed ($s^i_+ = s^{i+1}_-$) and that they are small in front of the plate's length ($d \ll L$). Following these assumptions, it is convenient to introduce lineic quantities defined by : $g = \mathcal{G}/d$, $l = \mathcal{L}d$, $q = Q/d$, and $v = V$. By using lineic quantities, the electrical charge displacement across a piezoelectric pair, and the added bending moment resulting from the inverse piezoelectric effect, are given as

$$q = \chi\theta' + cv, \qquad (1a) \qquad \mathcal{M}_{\text{piezo}} = -\chi v, \qquad (1b)$$

where χ is a mechanical/piezoelectric conversion coefficient and c is the lineic intrinsic capacity of a piezoelectric pair. The piezoelectric pair can thereby be considered as a capacitor and a current generator connected in parallel (see [2] for more details about the modeling of piezoelectric coupling). Thus together with the external RL circuit, the whole system is equivalent to a parallel RLC circuit connected to a current generator, and the charge conservation law of such a circuit is given by :

$$v + gl\dot{v} + l\ddot{q} = 0. \qquad (2)$$

In equations (1a, 1b, 2), $\dot{}$ and $'$ denote derivatives with respect to s and t, respectively.

In the following, the problem is nondimensionalized using $c_s = \sqrt{B/L^2\mu}$, the elastic wave velocity, as characteristic velocity. L, L/c_s, ρHL^2, $c_s\sqrt{\mu/c}$, $c_s\sqrt{\mu c}$ are respectively used as characteristic length, time, mass, voltage and lineic charge. As a result, 6 non–dimensional parameters characterize the coupled system :

$$M^* = \frac{\rho_f HL}{\mu}, \quad U^* = \frac{U_\infty}{c_s}, \quad H^* = \frac{H}{L}, \quad \alpha = \frac{\chi}{\sqrt{Bc}}, \quad \beta = \frac{cc_s}{gL}, \quad \omega_0 = \frac{L}{c_s\sqrt{lc}}.$$

M^* is a relative measure of the fluid and solid inertia. U^* is the reduced velocity representing the flow velocity, H^* the aspect ratio, α the piezoelectric coupling coefficient, and β and ω_0 represent respectively the conductance and the inductance. All variables are consequently taken non–dimensional hereafter, albeit denoted with the same letters as the dimensional ones.

3 Linear stability and threshold velocity

The flag in axial flow becomes unstable and starts to flutter when the reduced velocity exceeds a critical value U^*_{crit}. The dependence of this value on the mass ratio M^* and added conductance β, in case of resistive coupling, is observed in previous studies[5, 3, 7]. In this study, we are interested in the possible dependence of the U^*_{crit} on inductance, measured by ω_0. In order to study the influence of inductance, we consider linear configuration with a purely LC circuit by removing the second term in equation (2)

By considering small vertical displacement, i.e $y \ll 1$, we obtain the following linear equations for the coupled system :

$$\left(1 + \frac{\pi}{4}M^*H^*\right)\ddot{y} + \frac{\pi}{2}M^*H^*U^*\dot{y}' + \frac{\pi}{4}M^*H^*U^{*2}y'' + y'''' - \alpha v'' = 0, \qquad (3a)$$

$$\ddot{v} + \frac{1}{\beta}\dot{v} + \omega_0^2 v + \alpha\ddot{y}'' = 0 \qquad (3b)$$

with the linearized boundary conditions given by

$$\text{at } x = 0 : \; y = \dot{y} = 0, \qquad (4a)$$

$$\text{at } x = 1 : \; y'' - \alpha v = y''' - \alpha v' = 0 \qquad (4b)$$

We use a classical Galerkin decomposition method to study equations (3a, 3b) by assuming that the vertical displacement y is a linear combination of free vibration eigenmodes $\phi_i(x)$ of a cantilevered beam without coupling, while the voltage v is decomposed as a linear combination of $\phi_i''(x)$, since the latter verify the boundary conditions prescribed by (4a, 4b). The resulting decomposed equations are then projected onto $\phi_i(x)$ and $\phi_i''(x)$. Equations (3a–4b) are then recast as an eigenvalue problem and the coupled system is unstable if one of its eigenfrequencies has a positive imaginary part.

Threshold velocity U^*_{crit} is computed as a function of ω_0 for different values of M^* and shown in figure 3. We observe decreasing U^*_{crit} with increasing M^*. On the other hand, the influence of inductance is

observed when a given M^* is considered. In the limit $\omega_0 = 0$, the inductance is infinitely large so that the output circuit is equivalent to an open loop. Consequently, no charge transfer is possible within the circuit, and voltage in piezoelectric pairs is sufficiently high that an additional rigidity is induced to raise U^*_{crit} for all M^*. In the limit $\omega_0 \to \infty$, which corresponds to a very small inductance, each piezoelectric patch is directly shunted with the other one in the pair. Therefore, as explained in [3], voltage of each pair is nearly zero as a result of instantaneous charge transfer within the circuit. This case is equivalent to $\alpha = 0$, as no additional rigidity is induced.

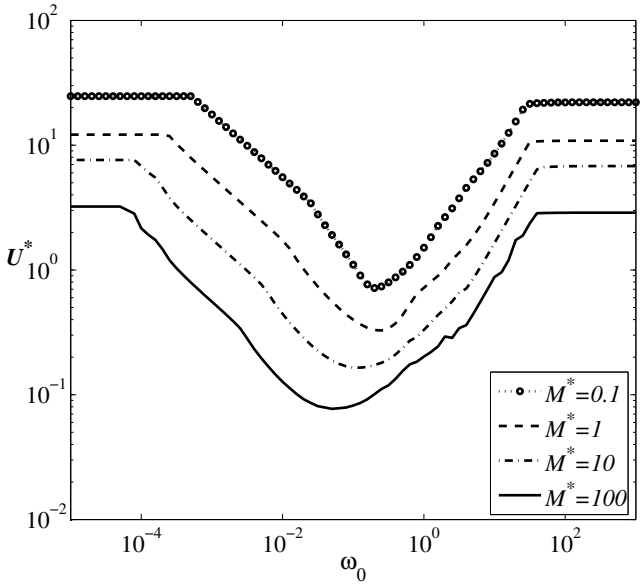

FIGURE 3 – Evolution of threshold velocity with ω_0 at $\alpha = 0.5$ and $H^* = 0.5$, with LC coupling

For intermediate ω_0, an important decrease of U^*_{crit} is observed for all M^*. The lowest U^*_{crit} is obtained with $\omega_0 \sim 0.1$ for all considered M^*. These results suggest some potential benefits of an output circuit with inductance, as it decreases the instability threshold, thus allowing energy harvesting by such mechanism with slow fluid flow or lighter fluid (e.g. using air instead of water)

4 Nonlinear dynamics

As predicted by linear stability theory, an unstable coupled system experiences, at initial stage, an exponential growth in its amplitude, which eventually saturates because of nonlinear effects. A complete study of the system's nonlinear dynamics is therefore necessary to evaluate the harvesting efficiency η, which is defined as the ratio between the power dissipated by the conductance g, and the kinetic energy flux of the fluid passing through the rectangular outlined by the width and peak–to–peak amplitude of the flag's trailing edge.

Non–dimensional equations describing the system's nonlinear dynamics are written as

$$\ddot{\mathbf{x}} = M^*(T\boldsymbol{\tau})' - (\theta''\mathbf{n})' + \alpha\left(v'\mathbf{n}\right)' + \mathbf{f}_{\text{fluid}}, \tag{5a}$$

$$\beta\ddot{v} + \dot{v} + \beta\omega_0^2 v + \alpha\beta\ddot{\theta}' = 0, \tag{5b}$$

$$\mathbf{f}_{\text{fluid}} = -m_a M^* H^* \left[\dot{u}_n - (u_n u_\tau)' + \frac{1}{2}u_n^2\theta'\right]\mathbf{n} - \frac{1}{2}M^* C_d |u_n| u_n \mathbf{n}, \tag{5c}$$

with the following boundary conditions

$$\text{at } x = 0: \ \mathbf{x} = \dot{\mathbf{x}} = 0, \tag{6a}$$

$$\text{at } x = 1: \ T = \theta' - \alpha v = \theta'' - \alpha v' = 0. \tag{6b}$$

In equations (5c), the drag coefficient C_d is 1.8 for a rectangular plate in a transverse flow. u_n and u_τ are respectively the normal and tangential components of the non–dimensional relative velocity of the flag to the flow. They are given, with non–dimensional variables, by :

$$u_n = -\dot{x}y' + \dot{y}x' + U^*y', \qquad (7a) \qquad u_\tau = \dot{x}x' + \dot{y}y' - U^*x'. \qquad (7b)$$

Equations (5a–5c) are solved using a method based on an explicit description of the fluid–solid coupling, introduced in [1], the only differences being that the fluid model is replaced in the present work by LAEBT, and that electric coupling is included. Frequency deviation is observed while studying

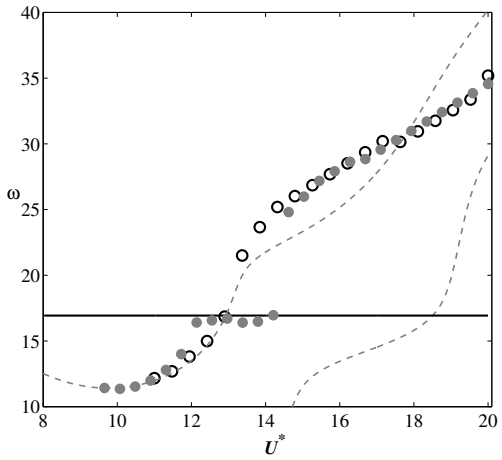

(a) Evolution of flapping frequency at $M^* = 1$ and $\omega_0 = 17$, for $\alpha = 0$ (black unfilled circles), $\alpha = 0.2$ and $\beta = 1$ (gray filled circles)

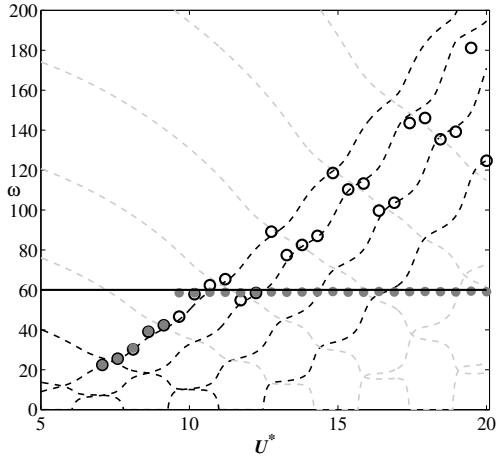

(b) Evolution of flapping frequency at $M^* = 10$ and $\omega_0 = 60$, for $\alpha = 0$ (black unfilled circles), $\alpha = 0.2$ and $\beta = 1$ (gray filled circles)

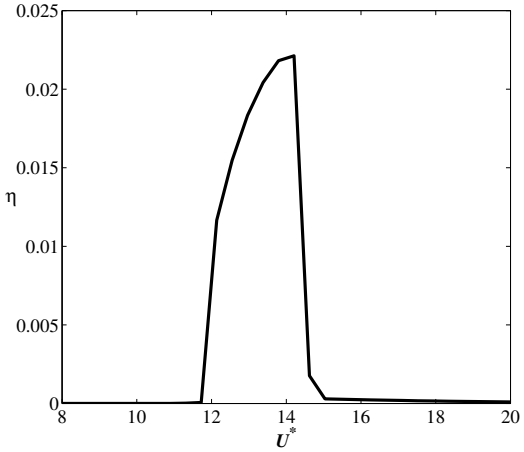

(c) Evolution of harvesting efficiency at $M^* = 1$, $\alpha = 0.2$ and $\beta = 1$

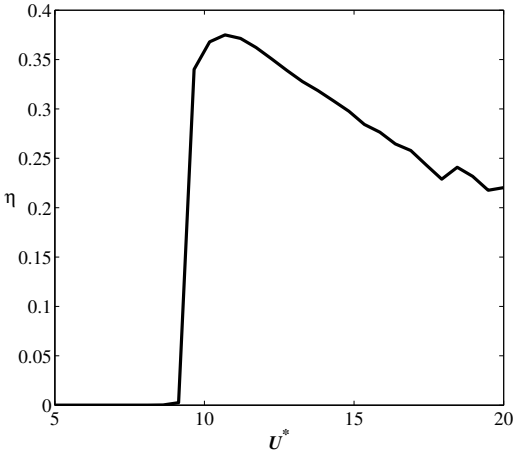

(d) Evolution of harvesting efficiency at $M^* = 10$, $\alpha = 0.2$ and $\beta = 1$

FIGURE 4 – Evolution of flapping frequency (a)(b) and harvesting efficiency (c)(d) with U^*. In both (a) and (b), ω_0 is represented by black solid lines. Dashed curves show linear modes frequencies evolution with U^*

nonlinear dynamics, as shown in figures 4a and 4b. It can be noticed that for both $M^* = 1$ and $M^* = 10$, when inductance is added ($\alpha \neq 0$), the flapping frequency no longer follows the frequency–velocity relation obtained without electric coupling ($\alpha = 0$). The flapping movement is actually dictated by

the output circuit, as the flapping frequency is very close to the natural frequency of the circuit, ω_0. A frequency lock–in phenomenon, as reported in some works on VIV (Vortex–Induced–Vibration)[8] is observed here, in which the frequency of one oscillator (the flag) is dictated by the frequency of the other (the circuit). For $M^* = 1$, lock–in with $\omega_0 = 17$ occurs with a certain range of U^* and disappears at higher U^*. For $M^* = 10$, lock–in with $\omega_0 = 60$ is observed for all U^* between 9.5 and 20. Moreover, lock–in seems not to be influenced by typical mode– switching events, which are indicated, for the uncoupled case, in figure 4b by transitions of flapping frequency between different linear modes.

With figures 4c and 4d, it is evident that the harvesting efficiency is strongly related to frequency lock–in. With both $M^* = 1$ and $M^* = 10$, harvesting efficiency increases significantly while the flapping frequency is deviated to ω_0. In particular, the maximal efficiency is around 0.02 with $M^* = 1$, and reaches almost 0.4 with $M^* = 10$. These results suggest a much higher energy harvesting performance compared with the case of a purely resistive output circuit [7].

5 Conclusion and perspectives

The present work studies the influence of inductive elements on the piezoelectric energy–harvesting flag. It was shown that the inductance can significantly destabilize the system, leading to an increase in the operation range of the device. The results on nonlinear dynamics showed the important role played by the RL circuit. We observed frequency lock–in occurred between the flapping flag and the circuit within a certain range of fluid velocity. The energy–harvesting efficiency is significantly increased while frequency lock–in occurs.

The above results indicate some potential benefits of the coupling of the energy–harvesting flag with complex electric systems. The critical role of the natural frequency of a circuit was identified. In the first place, a circuit possessing its own natural frequency introduces the possibility of resonance and frequency lock–in with the piezoelectric flag. As a consequence, energy–harvesting performance would be improved compared with the coupling with a purely resistive circuit. In the second place, the results of nonlinear study also suggested that, by carefully choosing a circuit's natural frequency, one might be able to control the flapping frequency regardless of the varying flow conditions. Although the simplest resonant circuit is used here, the results imply that by using more complex circuits with similar types of properties, substantial improvement in harvesting efficiency and controllability of the device can be expected.

Références

[1] S. Alben. Simulating the dynamics of flexible bodies and vortex sheets. *Journal of Computational Physics*, 228 :2587–2603, 2009.

[2] P. Bisegna, G. Caruso, and F. Maceri. Optimized electric networks for vibration damping of piezoactuated beams. *Journal of Sound and Vibration*, 289 :908–937, 2006.

[3] O. Doaré and S. Michelin. Piezoelectric coupling in energy-harvesting fluttering flexible plates : linear stability analysis and conversion efficiency. *Journal of Fluids and Structures*, 27(8) :1357 – 1375, 2011.

[4] C. Eloy, N. Kofman, and L. Schouveiler. The origin of hysteresis in the flag instability. *Journal of Fluid Mechanics*, 691 :583–593, 2012.

[5] C. Eloy, C. Souilliez, and L. Schouveiler. Flutter of a rectangular plate. *Journal of Fluids and Structures*, 23(6) :904 – 919, 2007.

[6] M. J. Lighthill. Large-amplitude elongated-body theory of fish locomotion. *Proceedings of the Royal Society, B*, 179 :125–138, 1971.

[7] S. Michelin and O. Doaré. Energy harvesting efficiency of piezoelectric flags in axial flows. *Journal of Fluid Mechanics*, 714 :489–504, 2013.

[8] C. H. K. Williamson and R. Govardhan. Vortex–induced vibrations. *Annual Review of Fluid Mechanics*, 36(1) :413–455, 2004.